Traffic & Transportation

Real-Time Scheduling Model for Shared Autonomous Vehicles in Ride-Sharing Mode

Shaoling RONG[1], Longxin ZENG[2], Fujian CHEN[3]

Original Scientific Paper
Submitted: 26 May 2025
Accepted: 19 Sep 2025
Published: 27 May 2026

[1] rongshaoling@163.com, College of Architecture and Transportation Engineering, Guilin University of Electronic Science and Technology, Guilin, China
[2] Corresponding author, 3447362588@qq.com, College of Architecture and Transportation Engineering, Guilin University of Electronic Science and Technology, Guilin, China
[3] chfj0102@guet.edu.cn, College of Architecture and Transportation Engineering, Guilin University of Electronic Science and Technology, Guilin, China

Publisher:
Faculty of Transport and Traffic Sciences, University of Zagreb

ABSTRACT
Numerous studies have demonstrated that ride-sharing optimisation for shared autonomous vehicles (SAVs) can effectively address the efficiency limitations of conventional shared mobility systems, realising the sustainable urban transportation vision of "serving more passengers with fewer vehicles". However, current shared autonomous vehicle (SAV) ride-sharing models exhibit inefficiencies. To overcome this, we propose a real-time SAV scheduling model with dynamic detour ride-sharing, minimising total passenger travel time while maximising ride-sharing distance ratios, thus fulfilling ride-sharing demands within defined spatial ranges. To solve this model, a two-stage ride-sharing scheduling matching approach was implemented, which integrates feasible matching pair acquisition and vehicle scheduling optimisation, with robustness and opportunism evaluated via Information Gap Decision Theory. MATLAB simulations validate the model by comparing dynamic detour ride-sharing with traditional overlapping modes. Results show the dynamic detour mode achieves a 64% ride-sharing rate using 68 vehicles, outperforming conventional modes with a 22% higher ride-sharing rate and 11 fewer vehicles required. This approach enhances ride-sharing adoption, alleviates congestion, lowers travel costs and maximises passenger service efficiency with minimal fleet size.

KEYWORDS
shared autonomous vehicles; dynamic detour ride-sharing; real-time scheduling; information gap decision theory.

1. INTRODUCTION

With the rapid development of the social economy, people's travel demand is steadily increasing. Traditional modes of transportation struggle to meet the diverse travel needs of people, necessitating the emergence of a new type of transportation that maximises the efficiency of limited resources – shared autonomous vehicles (SAVs) [1]. The rapid advancements in big data, the Internet of Vehicles, and artificial intelligence technology have continuously matured autonomous driving technology [2], [3]. By the end of the 21st century, autonomous vehicles are expected to be widely adopted. Coupled with the swift rise of the sharing economy, SAVs, which integrate autonomous vehicles with shared vehicle systems, are poised to become a novel travel mode. SAVs can offer dynamic ride-sharing services for self-driving taxis, enhancing travel flexibility [4]. Compared to traditional taxis, SAVs offer greater efficiency, environmental friendliness and personalisation. Since there is no subjective preference for drivers to choose orders, SAVs can unconditionally carry out passenger services according to schedule instructions, achieving true system optimisation in vehicle scheduling. However, the current ride-sharing models face the issue of low occupancy rates.

The ride-sharing service of SAVs can serve multiple passengers simultaneously, which is conducive to alleviating traffic congestion, reducing travel energy consumption and optimising vehicle resources [5]. To encourage passengers to share rides, improve scheduling efficiency and enhance the overall system revenue, it is necessary to formulate scientific and reasonable ride-sharing scheduling methods from the perspectives of both the operators of SAVs and the passengers. This can help reduce passengers' travel costs and lower travel energy consumption. Through literature retrieval, it is found that the current research on SAVs mainly focuses on two major fields: (1) the ride-sharing choice behaviour research; (2) the scheduling model of SAVs.

Existing research has systematically revealed the multidimensional driving mechanisms influencing shared autonomous vehicle (SAV) ride-sharing choice behaviour: at the framework level of influencing factors, sociodemographic variables (gender/age/income), attitudinal variables (technology acceptance/privacy concerns), behavioural variables (car-sharing experience/current vehicle automation level) and travel characteristic variables (congested areas/dedicated lanes) collectively form the decision-making foundation [6]. For instance, studies have identified user group differentiation manifested through higher acceptance rates among younger demographics, urban residents and more educated populations [7], [8]. The temporal-economic dimension demonstrates that travel time, waiting time and fare serve as core decision variables, with pickup/destination time reliability exhibiting threshold effects [9][10]. Grippenkoven et al. found that cost reduction potential from SAVs serves as a crucial incentive for urban residents to adopt such services [11]. Building on this, Pourgholamali et al. proposed a sustainability-driven policy framework for SAV-dedicated lanes and pricing strategies to minimise total travel time, trip costs, emissions and electricity consumption [12], [13]. Psycho-cognitive mechanisms identify technology acceptance [14] and comfort perception as key drivers, where personality traits [15] demonstrate greater predictive power than traditional socioeconomic attributes. Methodologically, the field has evolved from mixed logit models to ordered logit models, deepening the analysis of attitude-behaviour interaction mechanisms [16]. Ouaïl et al. [17] developed an agent-based model to simulate travellers' mode preferences between SAVs and existing options (e.g. private vehicles, public transit). Zhang et al. [18],[19] conducted simulation-based modal analyses comparing low-speed on-demand SAVs with existing short-distance mobility options.

The scheduling models of shared autonomous vehicles (SAVs) are intrinsically linked to the overall efficiency of SAV transportation systems and service quality. Although SAV ride-sharing may inconvenience individual passengers due to additional pickups, detours or delays, it significantly improves vehicle utilisation efficiency. Nourinejad et al. [20] developed a ride-sharing scheduling model for autonomous vehicles with dual objectives: minimising total vehicle mileage and maximising matching efficiency, while designing corresponding ride-matching algorithms. Subsequent simulations validated the model's performance. Mn et al. [21] formulated a network equilibrium framework to model multiple travellers sharing a single SAV, introducing a segmented user equilibrium model to characterise SAV traffic flow patterns. Liu [22] designs a zone-based dynamic clustering-driven multi-agent reinforcement learning (DC-MARL) model to tackle the limitations of current algorithms, which fail to effectively capture similar relocation actions through spatio-temporal relationships. Hyland et al. [23] proposed six intelligent optimisation strategies, demonstrating that their application reduces empty vehicle mileage and passenger wait times, particularly under high-demand conditions. Ge et al. [24] developed an SAV ride-sharing matching model, introducing a system-optimal traffic assignment framework to address the joint ride-matching and routing problem, leveraging a shareability network to facilitate route generation. Masoud et al. [25] examined the point-to-point ride-matching problem, employing dynamic programming to identify optimal SAV routes by minimising a linear combination of travel time, wait time and transfer frequency. Huang et al. [26] analysed the impact of SAVs as feeders to public transit, proposing a dynamic ride-matching algorithm that synchronises passenger arrivals at light rail stations with train schedules. Wang et al. proposed a two-stage optimisation framework integrating integer linear programming with genetic algorithms to achieve coordinated platooning of SAVs at urban intersections, demonstrating a 15.76% reduction in total SAV travel time while maintaining network-wide traffic efficiency in Shanghai's actual road network [27]. These studies collectively form the technological roadmap for SAV scheduling models evolving from single-objective optimisation to multimodal coordination.

Although existing research has achieved certain accomplishments in scheduling models and scheduling matching algorithms, the previous research results focused on the overlapping ride-sharing mode, which limited the starting and ending points of ride-sharing participants to the same route and did not consider the detour ride-sharing mode. The choice of ride-sharing was directly assumed without considering the ride-sharing preferences of passengers, nor the impact of traffic congestion on scheduling costs. Therefore, this study aims to propose a novel ride-sharing mode that balances operator profitability with passenger

preferences, delivering more flexible, efficient, eco-friendly and personalised shared mobility services. It will also effectively alleviate urban traffic congestion and environmental pollution. Building upon previous research, this study primarily makes the following contributions:

- The study innovatively proposes a "dynamic detour ride-sharing mode", which breaks through the limitations of traditional research that restricts ride-sharing paths to fixed routes. This mode dynamically optimises driving routes within passengers' maximum tolerable time range through an elastic path planning algorithm, while parameterising passenger preferences and integrating them into the cost function, achieving a synergistic optimisation of operational efficiency and passenger satisfaction.
- The study constructs a model based on multi-objective optimisation. The model develops a dynamic preference feature extraction mechanism. Through the objective function design, it achieves precise alignment between scheduling parameters and passenger demands. Compared to the static preference assumptions used in existing research, this model keeps detour ride-sharing times within passengers' acceptable ranges, improving the practicality and human-centric nature of the scheduling system.
- The study introduces Information Gap Decision Theory (IGDT) into the field of SAV dynamic scheduling. By constructing a dual-mode evaluation system that includes both robust and opportunistic models, the impact of travel time fluctuations on scheduling stability is addressed. This provides an innovative solution for the reliable operation of SAVs in a complex urban traffic environment.

The framework of this study is structured as follows. The first section clarifies the background, current status and challenges. The second section focuses on constructing a real-time scheduling model for ride-sharing, encompassing model assumptions, objective function design and constraint formulation. Innovatively, IGDT is introduced to analyse model robustness, alongside a two-stage solution approach (feasible matching pair acquisition and vehicle scheduling optimisation). The third section validates the model's effectiveness through simulation experiments, with comparative analysis of key metrics across different modes. The fourth section conducts parameter sensitivity analysis, examining the impact of uncertainty parameters and cycle duration. Finally, the study summarises the findings, demonstrating the efficacy of the dynamic detour ride-sharing mode and proposing novel insights for intelligent transportation scheduling.

2. MODEL FORMULATION AND SOLUTION

2.1 Problem description

SAVs can realise intelligent travel control, unconditionally follow the scheduling arrangement of the scheduling system, and respond to the scheduling scheme in real time according to the instructions of the scheduling system. By analysing passengers' travel needs and ride-sharing preferences, personalised matching between passengers can be achieved. From the perspective of system optimisation, it accurately realises the dynamic ride-sharing between passengers from point to point, and provides high-quality ride-sharing services. The SAV ride-sharing scheduling problem studied in this paper refers to that there are multiple SAVs in the road network, some vehicles are driving in the road network, and some vehicles are waiting at the parking station. Passengers send a ride-sharing request to the scheduling system through smartphones and other network devices. The request content includes: passengers' starting and ending points, taxi time, the maximum acceptable ride time, the number of seats required, and personal attribute preferences for the ride-sharing object. The scheduling system analyses the information requested by passengers, and realises the passenger-to-passenger or passenger-to-vehicle ride-sharing matching scheme according to the ride-sharing scheduling matching solution, and sends the ride-sharing matching scheme to the SAVs' terminal. If there are multiple passengers in a request, they are considered as a whole. The dispatching system uses the periodic rolling update mechanism to arrange the service for new passengers. If the new passengers do not match successfully in one cycle, they will be transferred to the next cycle. If the matching is not successful, empty vehicles will be arranged for service, including empty vehicles running in the road network and waiting at the parking station.

2.2 Model assumptions

- Assumption 1: In a ride-sharing service, each SAV can accept up to two ride-sharing requests, and the number of passengers in the vehicle does not exceed three.
- Assumption 2: Passengers in the same request have the same starting and ending points, i.e. boarding and alighting at the same time.

— Assumption 3: The SAV is uniformly scheduled by the scheduling system, and can be served all day, and can fully comply with the instructions of the scheduling system.
— Assumption 4: The additional detour costs incurred by passengers participating in the ride-sharing will not be counted, and corresponding discounts will be given to the ride costs.

2.3 Model establishment

Model symbols and definition

To facilitate the description of the model, the following symbols and their definitions are listed in *Table 1*.

Table 1 – Definitions of model symbols

Symbols	Definitions
G	A complete directed network, $G=(N, E, K, R)$
N	The set of points, $N'=\{O, D, U \mid N' \subset N\}$
O	The sets of starting points of passengers
D	The sets of ending points of passengers
U	The sets of current positions of vehicles
E	The set of edges. $i, j \in N$, $E=\{(i, j) / i, j \in N, i \neq j\}$, and $e(i, j)$ denote an edge for a vehicle to travel from point i to point j
K	The vehicle set, $k=\{(u_k, t_i^k, F_k, F_i^k, T_i) / k \in K\}$
u_k	The current position of the vehicle, $u_k \in U$
t_i^k	The time it takes for vehicle k to travel from its current position u_k to the request starting point i
t_{ij}^k	The time taken by vehicle k to travel from point i to point j while carrying passengers, which can represent passengers' in-vehicle time
F_k	The maximum vehicle capacity
F_i^k	The remaining seats of vehicle k before leaving the departure point i
g_i^k	The passenger occupancy of vehicle k upon arrival at node i, serving as a critical constraint to ensure the actual load never exceeds the maximum capacity F_k
T_i	The time when the vehicle arrives at point i
R	The passenger request set, $r=\{(o_r, d_r, T_r, q_r, t_r^*) / r \in R\}$
o_r	The departure location, $o_r \in O$
d_r	The destination location, $d_r \in D$
T_r	Maximum tolerable in-vehicle travel time threshold
q_r	The seat capacity requirement (taking integer values ≥1, e.g., q_r= 2 for two passengers travelling jointly)
t_r^*	The theoretical minimum trip duration derived from unimpeded point-to-point travel time under free-flow conditions

Objective function

1) The total travel time cost for passengers is minimised

The operating cost of the vehicle is mainly the fuel consumption and depreciation cost during the driving process of the vehicle, and the fuel consumption is directly proportional to the running time of the vehicle. The total travel time of passengers refers to the in-car time of all passengers. The less the total travel time of passengers, the less the running time of vehicles, which is more conducive to cost saving. The objective function of minimising the total travel time cost of passengers is:

$$min \sum_{k \in K} \sum_{i, j \in N} t_{ij}^k x_{ij}^k \tag{1}$$

In *Equation (1)*, N is the node in the road network, x_{ij}^k is the decision variable. When the vehicle moves from node i to node j, x_{ij}^k takes 1, and vice versa.

2) The ride-sharing distance ratio is maximised

The ride-sharing distance ratio $p_{2\le\lambda_r\le3}$ refers to the proportion between: **(a)** the actual distance travelled during shared rides when the number of passenger $2\le\lambda_r\le3$, and **(b)** the total route distance required to sequentially deliver all passengers from the current location u_k to their respective destinations. To make full use of road resources and reduce the travel cost of passengers, this study takes the ride-sharing distance ratio as another objective function. Under the constraints of the model, the greater the ratio of the ride-sharing distance, the greater the value of the combined ride matching. The objective function of the maximum ratio of the ride-sharing distance is:

$$max \sum_{r\in R} p_{\lambda_r},\ 2\le\lambda_r\le3 \tag{2}$$

Considering a two-passenger ride-sharing scenario $\lambda_r=2$ with fixed boarding order ($r_1\rightarrow r_2$), the ride-sharing distance ratio requires two unique formulations corresponding to possible alighting sequences:

$$p_{\lambda_r=2}=\begin{cases} dis(o_{r_2}, d_{r_1})/dis(u_k, d_{r_2}) & , \text{alighting sequences: } r_1\rightarrow r_2 \\ dis(o_{r_2}, d_{r_2})/dis(u_k, d_{r_1}) & , \text{alighting sequences: } r_2\rightarrow r_1 \end{cases} \tag{3}$$

Considering a three-passenger ride-sharing scenario $\lambda_r=3$ with fixed boarding order ($r_1\rightarrow r_2\rightarrow r_3$), the ride-sharing distance ratio requires six unique formulations corresponding to possible alighting sequences:

$$p_{\lambda_r=3}=\begin{cases} dis(o_{r_2}, d_{r_2})/dis(u_k, d_{r_3}) & , \text{alighting sequences: } r_1\rightarrow r_2\rightarrow r_3 \\ dis(o_{r_2}, d_{r_3})/dis(u_k, d_{r_2}) & , \text{alighting sequences: } r_1\rightarrow r_3\rightarrow r_2 \\ \cdots & \\ dis(o_{r_2}, d_{r_2})/dis(u_k, d_{r_1}) & , \text{alighting sequences: } r_3\rightarrow r_2\rightarrow r_1 \end{cases} \tag{4}$$

It should be specifically noted that: **(a)** For ease of description, both *Equation (3)* and *Equation (4)* assume that each passenger request involves only one passenger (i.e. single occupancy per request). **(b)** In *Equation (4)*, the vehicle must carry exactly three passengers per trip, meaning we exclude cases where a passenger alights before the third passenger boards.

Constraint conditions

1) Time-window constraint

Each passenger participating in the ride-sharing shall be picked up and sent within the specified time, and the travel time of passengers shall not exceed the maximum ride time they can accept.

Waiting time of passengers:

$$0\le tor\ k\le 5min, \forall r\in R,\ k\in K \tag{5}$$

Travel time of passengers:

$$T_{d_r}-T_{o_r}\le T_r, \forall r\in R \tag{6}$$

2) Vehicle capacity constraint

The number of passengers in the running process of the vehicle shall not exceed the maximum capacity of the vehicle. When the scheduling system carries out ride-sharing scheduling matching, the number of remaining seats shall meet the number of seats requested by passengers.

$$1\le q_r\le F_i^k, \forall k\in K,\ r\in R,\ i\in O\cup D \tag{7}$$

$$0\le g_i^k\le 3, \forall i\in N,\ k\in K \tag{8}$$

3) Ride-sharing preference constraint

Because passengers have different preferences for the gender of the ride-sharing partner, this constraint should be taken into account when the scheduling system performs the scheduling matching.

$$G_{r_1}=ok \tag{9}$$

$$G_{r_2}=ok \tag{10}$$

Equations (9) and *(10)* formally establish gender preference compatibility constraints between ride-sharing participants: **(a)** primary passenger r_1: the initially boarded passenger's gender preference; **(b)** secondary passenger r_2: subsequently boarded passenger's gender preference.

Parameter $\theta \in \{1,2,3,4\}$ is introduced to encode passengers' gender preference types for ride-sharing (*Table 2*). Suppose that:

Table 2 – Definitions of passengers' gender preference types

θ	Gender preference type
1	A female passenger needs to be matched with another female passenger
2	A female passenger has no requirements for the gender of the ride-sharing partner
3	A male passenger needs to be matched with another male passenger
4	A male passenger has no requirements for the gender of the ride-sharing partner

The matching scenarios are as follows (*Table 3*):

Table 3 – Matching scenario types

$r_1(\theta)$	$r_2(\theta)$
$r_1(\theta=1)$	$r_2(\theta \in \{1,2\})$
$r_1(\theta=2)$	$r_2(\theta \in \{1,2,4\})$
$r_1(\theta=3)$	$r_2(\theta \in \{3,4\})$
$r_1(\theta=4)$	$r_2(\theta \in \{2,3,4\})$

4) Other constraints

$$\sum_{k \in K} y_r^k \leq 1, \ \forall r \in R \tag{11}$$

$$\sum_{r \in R} y_r^k \leq 1, \ \forall k \in K \tag{12}$$

$$\sum_{i \in N} f_i^k \leq 1, \forall k \in K \tag{13}$$

$$\sum_{j \in N'} x_{ij}^k = 1 \ \forall i \in O \cup D, \ k \in K \tag{14}$$

$$\sum_{i \in N^+(j)} x_{ij}^k = \sum_{i \in N^-(j)} x_{ji}^k = 1, \forall i,j \in N', k \in K \tag{15}$$

$$\sum_{i \in N^-(o_r)} x_{o_r i}^k \geq y_r^k, \sum_{i \in N^+(d_r)} x_{i d_r}^k \geq y_r^k, \forall k \in K, r \in R \tag{16}$$

$$x_{ij}^k \in \{0,1\}, \ y_r^k \in \{0,1\}, \ f_i^k \in \{0,1\}, \forall i,j \in N \tag{17}$$

Equation (11) indicates that each SAV can only conduct one matching within a cycle. *Equation (12)* means that a passenger can be served by at most one SAV. *Equation (13)* shows that an SAV will automatically return to the parking site when it has no service. *Equations (14)* and *(15)* ensure the balance of vehicle flow in and out of points i and j. *Equation (16)* restricts the vehicle flow at the passenger boarding and alighting points. *Equation (17)* presents the decision variables. $x_{ij}^k \in \{0,1\}$ represents that if a vehicle travels from point i to point j, then x_{ij}^k

takes the value of 1; otherwise, it takes 0. $y_r^k \in \{0,1\}$ means that if k serves r, then y_r^k takes the value of 1; otherwise, it takes 0. $f_i^k \in \{0,1\}$ means that if a vehicle has no service, then f_i^k takes the value of 1; otherwise, it takes 0.

2.4 Robustness and opportunity of the real-time dispatching model based on Information Gap Decision Theory (IGDT)

The Information Gap Decision Theory (IGDT) was proposed by Ben-Haim in 2001. It is an optimisation method that can effectively handle the uncertain factors in a system. Here, "information" refers to the information of uncertain factors that affect the system's objectives, and "gap" refers to the difference between the predicted value and the actual value of the uncertain factors. This method does not require the probability distribution function and membership function of the uncertain factors, making it suitable for use in scenarios with high uncertainty or a large lack of uncertain information [28].

The uncertainty and complexity of traffic flow make it difficult to capture uncertain information, such as people's travel times. The IGDT model provides a theoretical basis for this paper to study the impact of the uncertainty of passengers' travel times on travel time costs.

Rewrite the part of the real-time scheduling model of SAVs under the ride-sharing mode in this paper, which aims at the total travel time of passengers, into vector form, as shown in *Equation (18)*.

$$\begin{cases} \min T(v, t_{ij}) \\ s.t\ \ H(v, t_{ij}) = 0, \forall i,j \in N \\ G(v, t_{ij}) \le 0 \end{cases} \tag{18}$$

In *Equation (18)*, T represents the objective function of the total travel time of passengers; v is the decision-making variable; $H(v,t_{ij}) = 0$ and $G(v,t_{ij}) \le 0$ are the equality constraint and inequality constraint conditions of the real-time scheduling model respectively.

Model the uncertainty of passengers' travel time t_{ij}, and its expression is shown in *Equation (19)*.

$$\begin{cases} t_{ij} \in W(\alpha, t_{ij}^*) \\ W(\alpha, t_{ij}^*) = \{t_{ij} : |(t_{ij} - t_{ij}^*) / t_{ij}^*| \le \alpha, \forall i,j \in N\} \\ 0 \le \alpha \end{cases} \tag{19}$$

In *Equation (19)*, t_{ij}^* is the predicted value of t_{ij}. α represents the uncertainty degree of the passengers' travel time t_{ij}. W represents the difference of t_{ij}. This equation indicates that the maximum difference between t_{ij} and t_{ij}^* is $\pm\alpha t_{ij}^*$.

Considering the different risk preferences of decision-makers when making decisions, the corresponding robustness model (RM) and opportunity model (OM) are constructed, and their expressions are shown in *Equations (20)* and *(21)*.

$$\begin{cases} \max \alpha^{RM} \\ s.t\ \ \max T(v, t_{ij}) \le (1+\beta^{RM}) T_0 \\ \forall x \in W(\alpha, t_{ij}^*) \\ Equations(5) - Equations(17) \end{cases}, \forall i,j \in N \tag{20}$$

$$\begin{cases} \min \alpha^{OM} \\ s.t\ \ \min T(v, t_{ij}) \le (1-\beta^{OM}) T_0 \\ \forall x \in W(\alpha, t_{ij}^*) \\ Equations(5) - Equations(17) \end{cases}, \forall i,j \in N \tag{21}$$

The robustness model (RM) transforms the objective of the total travel time of passengers in the real-time scheduling model into the maximum uncertainty radius α^{RM} that ensures the total travel-time cost meets the requirement of being no greater than the expected value $(1+\beta^{RM})T_0$. That is, in the case where there is significant uncertainty in travel times, the RM calculates the decision value v. When the input parameter t_{ij} fluctuates within the range W, it can still guarantee that the objective value does not exceed the expected value

$(1+\beta^{RM})T_0$. A larger value of α^{RM} obtained from the RM indicates that the decision-making scheme is less sensitive to the uncertainty of the parameters, i.e. it has better robustness.

The opportunity model (OM) transforms the objective of the real-time scheduling model into determining the minimum uncertainty level α^{OM} that satisfies the condition where travel time costs do not exceed the expected value $(1-\beta^{OM})T_0$. Specifically, under conditions of significant travel time uncertainty, the opportunity model derives an optimal decision variable v that guarantees the target value remains no worse than the performance threshold W when input parameters t_{ij} fluctuate within the bounded range $W(\alpha,t_{ij}^*)=(1-\beta^{OM})T_0$.

In *Equations (20)* and *(21)*, β^{RM} and β^{OM} represent the cost deviation factors set by the decision-maker, which are the deviations of the expected cost from the baseline value, either higher or lower, respectively.

Solution steps for the real-time scheduling model of SAVs based on IGDT:

— Solve the objective values of the real-time scheduling model to obtain the baseline values T_0 and P.

— Set the cost deviation factors β^{RM} and β^{OM}, and calculate the expected target values $(1+\beta^{RM})T_0$ and $(1-\beta^{OM})T_0$ of the robustness model and the opportunity model that the decision-maker can accept.

— Calculate the uncertainty radii α^{RM} and α^{OM} and the target values of the robustness model and the opportunity model, respectively.

2.5 Solution method

Solution process

The real-time scheduling of SAVs under the ride-sharing mode is a scheduling problem where the states of vehicles and passengers change over time. At the beginning of the system operation, the system executes an initialisation procedure for the existing passenger requests. Each passenger is randomly matched with an SAV, and the initial routes are generated accordingly. However, as time passes, the system will receive new ride-sharing requests from passengers, and the states of the vehicles will change continuously. The scheduling system needs to dynamically match real-time passenger request information with SAVs in the road network. From the perspective of system optimality, it should provide the optimal scheduling and matching scheme in real-time. To solve the problem of dynamic ride-sharing of SAVs over time, this paper sets the cycle duration as t_0 and divides the period into M cycles. A cycle-rolling update mechanism is adopted to update dynamic information such as vehicle status information and passenger travel information. The solution method for the real-time scheduling model of SAVs under the ride-sharing mode proposed in this paper is divided into two stages: obtaining feasible matching pairs and optimising vehicle scheduling and matching. The overall flowchart of the solution method is shown in *Figure 1*.

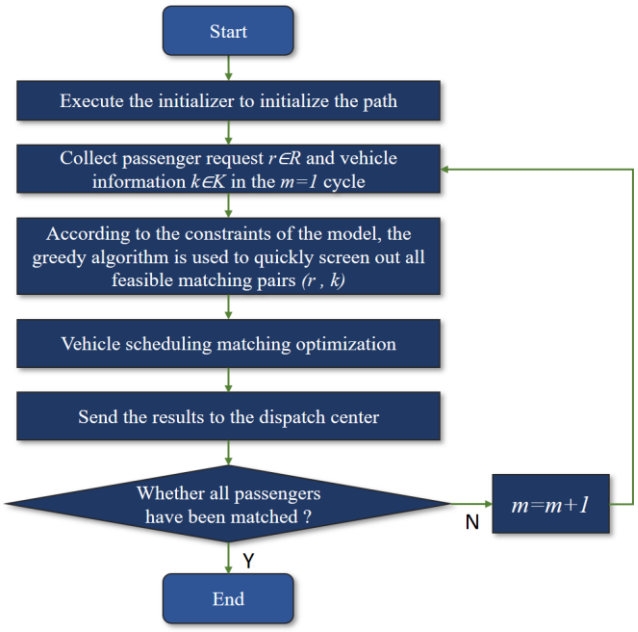

Figure 1 – Flowchart of solutions for real-time scheduling model

Feasible matching pairs acquisition

Passengers can be matched with SAVs in four states: currently shareable SAVs, expectedly shareable SAVs, currently empty SAVs and expectedly empty SAVs. Currently, shareable SAVs refer to vehicles with only one passenger inside, that is, vehicles whose remaining seat number meets the requirement of $1 \le F_i^k \le 2$. These vehicles can share the journey with other passengers. Expectedly shareable SAVs are those that currently have no remaining seats, meaning the expected remaining seat number meets the requirement of $1 \le F_i^k \le 2$. After one or two passengers get off, the remaining passengers can then share the journey with other passengers. Currently empty SAVs are vehicles that are not currently occupied by any passengers. Expectedly empty SAVs are occupied vehicles that will serve new passengers after the current passengers get off, that is, vehicles whose expected remaining seat number meets the requirement of $F_i^k = 3$. This study only considers currently shareable SAVs and currently empty SAVs, and gives priority to currently shareable SAVs when the constraint conditions are met.

When the SAV scheduling centre receives a passenger's request, the system, centred around the passenger, searches for SAVs within a 3-kilometre radius to match with the passenger based on the passenger's request information, to obtain feasible matching pairs. The specific process is shown in *Figure 2*.

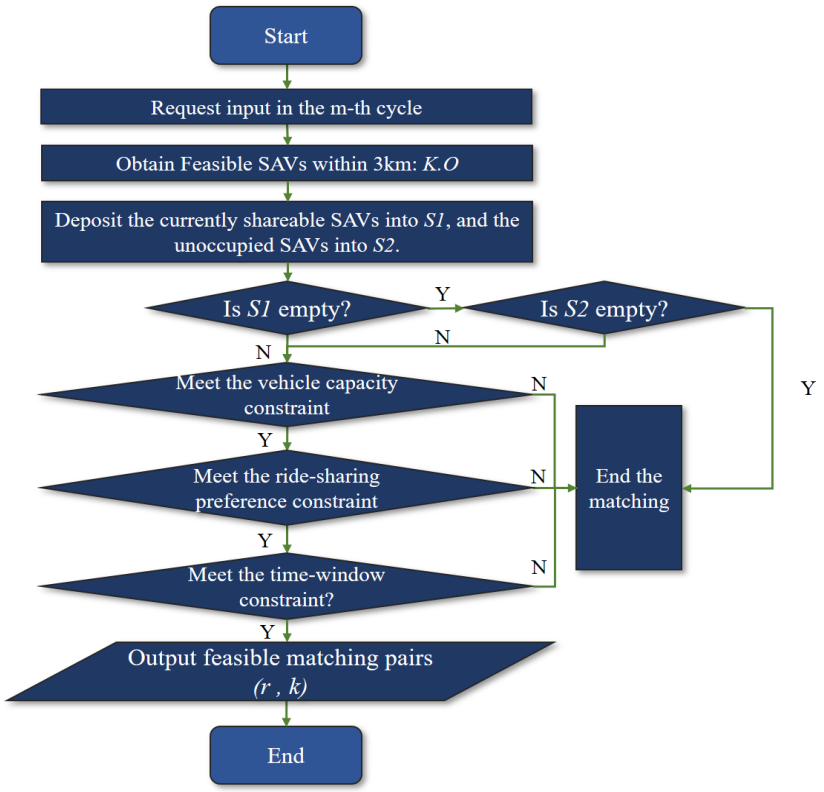

Figure 2 – Flowchart for obtaining feasible matching pairs

First, conduct checks on the vehicle capacity constraint and ride-sharing preference constraint for the obtained SAVs, and screen out the vehicles that meet the number of seats required by the passenger's request and the passenger's ride-sharing preferences. Then, use the greedy insertion method to check the time-window constraint and determine whether any vehicle that meets the vehicle capacity and ride-sharing preference constraint and any passenger request can form a feasible matching pair. The judgment idea is as follows.

Assume that currently, a SAV is serving passenger 1 from the starting point o_1 to the destination d_1. Then, the initial insertion order of the starting and ending points o_2 and d_2 of new passenger 2 is (o_2, d_2, d_1). If (o_2, d_2, d_1) meets the model's constraint conditions, the insertion is terminated, indicating that passenger 1 and passenger 2 can form a feasible matching pair; otherwise, the insertion order is changed. If continuing to insert in the order of (o_2, d_1, d_2) still fails to meet the constraint conditions, it means that this vehicle cannot serve the new passenger 2, and the insertion is terminated. If a new passenger 2 cannot be matched with currently shareable SAVs in the road network, the surrounding empty vehicles are selected for further judgment. If an empty vehicle meets the passenger's waiting-time constraint condition, it is arranged to serve the passenger.

The final ride-sharing route for passenger 1 and passenger 2 is determined by the scheduling and matching algorithm of the model. Any passenger request can form feasible matching pairs with multiple SAVs, and any SAV can form feasible matching pairs with multiple passenger requests, as shown in *Figure 3*.

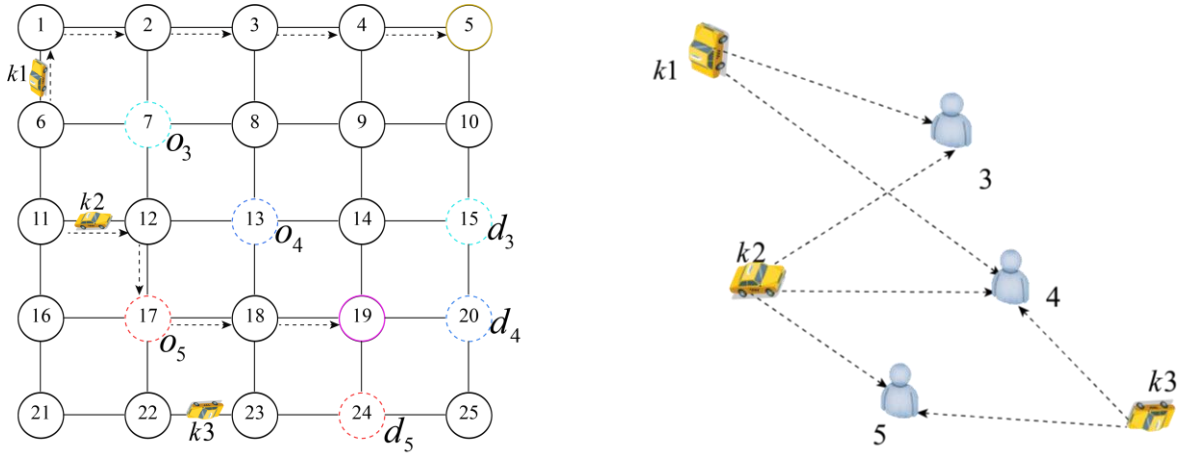

(a) *(b)*

Figure 3 – Obtaining of feasible matching pair: a) Original distribution of vehicles and passenger requests; b) Vehicle-passenger matching situation

In *Figure 3(a)*, assume that there are three passenger requests in the road network within one cycle. Here, o_1、o_2、o_3 represent the starting points of passenger request 3, passenger request 4 and passenger request 5, respectively, and the corresponding destinations of these passenger requests are d_1、d_2、d_3. Based on the passenger request information, it is found that there are three SAVs in the road network. Among them, vehicle *k1* has passenger 1 on board, vehicle *k2* has passenger 2 on board, and these two vehicles initially travel along their original planned routes. Vehicle *k3* is an empty vehicle. *Figure 3(b)* shows all the feasible matching pairs between passenger requests and SAVs within this cycle. Vehicle *k1* can form a feasible matching pair with both passenger request 3 and passenger request 4. Vehicle *k2* can form feasible matching pairs with all three passenger requests, and vehicle *k3* can form feasible matching pairs with passenger request 4 and passenger request 5. The final scheduling and matching scheme will be determined by the vehicle scheduling and matching optimisation method described in the next section.

Vehicle scheduling matching optimisation

1) Matching optimisation process

Through the stage of obtaining feasible matching pairs, all the feasible matching pairs between $r \in R$ and $k \in K$ and their corresponding trips within one cycle are finally obtained, which are represented by (r, k) and T_{tr} respectively, and ultimately form $T_{tr}=\{(r, k)=\{t, T_t, P_t\} | r \in R, k \in K\}$. Each feasible matching pair corresponds to a trip t. Therefore, when vehicle k completes trip t, it means that it serves request r. Each travel request may have multiple feasible matching pairs, and each feasible matching pair is completed by different vehicles. The algorithm flow of this matching optimisation process is shown in *Figure 4*.

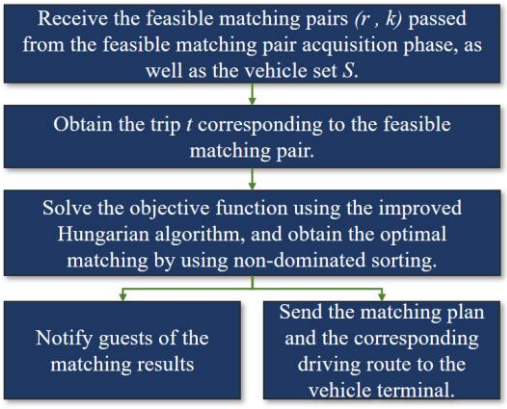

Figure 4 – Flowchart for scheduling and matching optimisation of SAVs

Let T_{tr}^{k} be the set of trips served by vehicle k, T_{tr}^{r} represent the set of trips where passenger request r is located, T_{tr}^{*} be the set of all trips, S be the set of vehicles k that can serve request r, and $\varepsilon_{t,k}=\{0,1\}$ be the decision-making variable for trips. When $\varepsilon_{t,k}=1$, it indicates that trip t is completed by vehicle k; otherwise, its value is 0. When $\varphi_r=1$, it means that passenger r 's request fails; otherwise, its value is 0. Each request is served by at most one SAV, and each SAV conducts at most one matching within a cycle. With the goals of minimising the total travel-time cost of passengers and maximising the ratio of ride-sharing distances, the final trips are determined through the matching optimisation method.

$$min \sum_{t \in T_{tr}^{*}} \sum_{k \in S} T_t \, \varepsilon_{t,k} \tag{22}$$

$$max \sum_{t \in T_{tr}^{*}} \sum_{k \in S} P_t \, \varepsilon_{t,k} \tag{23}$$

$$\sum_{t \in T_{tr}^{k}} \varepsilon_{t,k} \leq 1, \forall k \in K \tag{24}$$

$$\sum_{t \in T_{tr}^{r}} \sum_{k \in S} \varepsilon_{t,k} + \varphi_r = 1, \forall r \in R \tag{25}$$

Equation (22) is the objective function for the total travel-time cost of passengers. This objective function aims to minimise the total travel-time cost, ensuring that passengers are delivered to their destinations in the shortest possible time. *Equation (23)* is the objective function for the ratio of ride-sharing distances of passengers, which is designed to maximise this ratio. *Equations (24)* and *(25)* are the constraint conditions. *Equation (24)* stipulates that each SAV can only conduct one matching within a cycle, and *Equation (25)* indicates that each passenger can be served by at most one SAV.

2) Matching optimisation algorithm

The scheduling of shared autonomous vehicles in the ride-sharing mode belongs to the assignment problem. The assignment problem refers to the situation where X individuals are required to complete Y tasks, and the task assignment scheme is determined based on the efficiency of each individual in completing various tasks to ensure that the work is completed with the best efficiency. For the assignment problem, the most standard and classic solution algorithm is the Hungarian algorithm (HA). Inspired by mathematician Konig's theorem on independent zero-elements in matrices, scholar Kuhn proposed the traditional Hungarian algorithm, which is a standard algorithm specifically for the assignment problem [29]. The traditional Hungarian algorithm has a relatively narrow scope of application and is limited to one-to-one assignment problems. Subsequently, scholars used the "edge-adding and zero-filling method" to transform the solution matrix into a square matrix, converting the traditional HA into an adaptive HA to solve the task assignment problems where the number of tasks is less than or greater than the number of workers [30]. This algorithm is easy to understand and can quickly obtain the optimal assignment scheme. Therefore, this paper uses the improved Hungarian algorithm to optimise the vehicle ride-sharing matching.

3. MODEL AND SOLUTION VALIDATION

3.1 Design of experimental simulation scheme

In this paper, the simulation experiment road network is the Sioux Falls road network, as shown in *Figure 5*. This road network has a total of 24 road intersection nodes, 42 in-road nodes and 72 directed road segments. The blue-coloured numbers represent the lengths of the road segments. The road network in *Figure 5(a)* does not include in-road nodes, while the road network in *Figure 5(b)* includes all nodes. The experimental simulation is carried out using MATLAB 2018b, and the experimental simulation environment is equipped with an Intel Core i7-8700 processor, with a clock speed of 3.20 GHz and 8 GB of RAM.

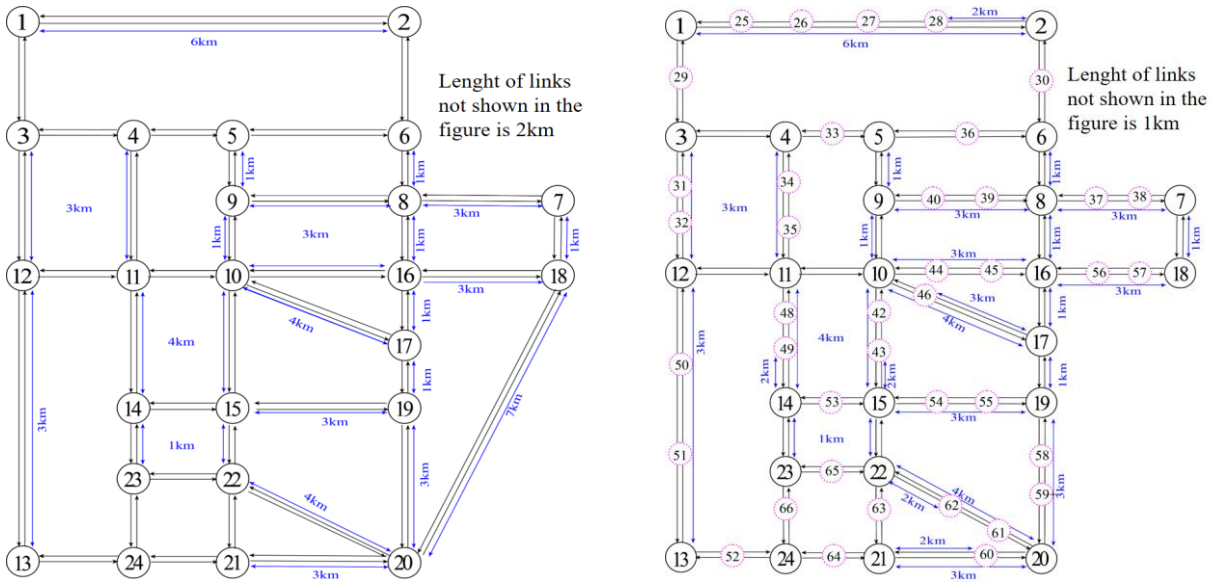

(a) *(b)*

Figure 5 – Sioux Falls road network

The experimental data are derived from the OD travel demands of the Sioux Falls road network. A total of 100 OD travel demands are obtained, and the Floyd algorithm is used to pre-calculate the shortest distances between each pair of points. The initial positions of the vehicles are set at node 10 in *Figure 5*, and the number of vehicles is 80. At the beginning of the system operation, an initialisation procedure is executed. A certain portion of passengers and vehicles are randomly matched to form the initial vehicle routes, which are shown in *Table 4*. The vehicles travel at a constant speed of 60 km/h. The value of t_0 is set to 60 seconds, and M is set to 50.

Table 4 – Initial path table

Number	Initial path
1	10→9→8→6→5→4→3→1
2	10→11→14
3	10→11→4→5→6→8
4	10→9→5→9→10→15
5	10→11→14→23→22
6	10→11→12→11→14→15
7	10→15→22→23→24→13
8	10→9→8→16→18
9	10→16→17→19→20
10	10→17→16→8→6→5→4

3.2 Analysis of experimental simulation results

Analysis of ride-sharing rates and the number of required vehicles for different ride-sharing modes

This paper takes into account two dynamic ride-sharing modes, namely the dynamic detour ride-sharing mode and the overlapping ride-sharing mode, and conducts experiments. The ride-sharing rates and the number of required vehicles for the two modes are calculated, respectively, and the experimental results are shown in *Figure 6*. The ride-sharing distribution of passengers in the dynamic detour mode is shown in *Figure 7*.

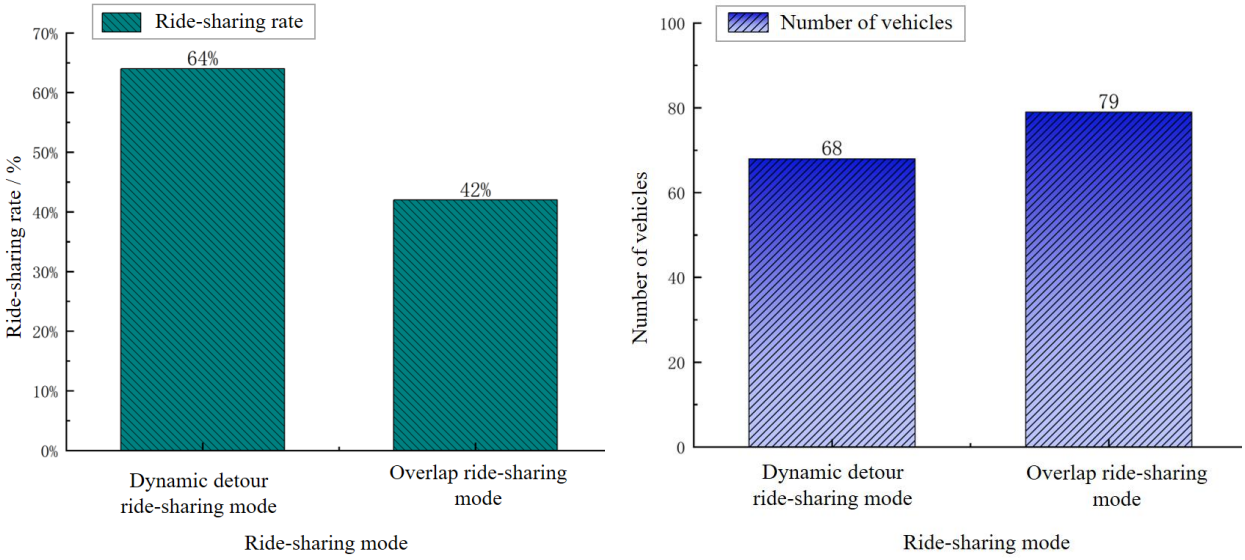

(a) *(b)*

Figure 6 – Scheduling results of different multiplicative modes: a) Ride-sharing rate of different ride-sharing modes; b) Number of vehicles with different ride-sharing modes

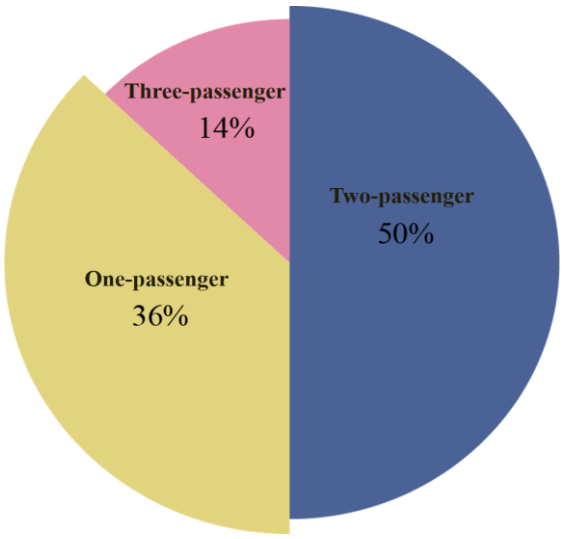

Figure 7 – Passenger ride-sharing distribution

As can be seen from *Figure 6*, the ride-sharing rate of passengers in the dynamic detour ride-sharing mode is 64%, while that in the overlapping ride-sharing mode is 42%. Compared with the overlapping ride-sharing mode, the ride-sharing rate in the dynamic detour ride-sharing mode is increased by 22%. In the dynamic detour ride-sharing mode, the actual total number of required vehicles is 68, and in the overlapping ride-sharing mode, it is 79. Compared with the overlapping ride-sharing mode, the actual total number of required vehicles in the dynamic detour ride-sharing mode is reduced by 11. As shown in *Figure 7*, in the dynamic detour mode, the proportion of three-passenger rides is 14%, and the proportion of two-passenger rides is 50%. Through the experiment, it is found that the ride-sharing rate of passengers in the dynamic detour ride-sharing mode is higher than that in the overlapping ride-sharing mode, and the ride-sharing efficiency is significantly improved, indicating that both the model and the solution method are effective.

On the premise of meeting the detour ride-sharing mileage, the dynamic detour ride-sharing mode provides a more flexible ride-sharing route, not limited to the same origin-destination. The dynamic detour ride-sharing mode will provide more passengers with opportunities for ride-sharing travel. With the same number of travellers, as the number of passengers participating in ride-sharing increases, the number of required vehicles will decrease. Therefore, dynamic detour ride-sharing can serve more passengers with fewer vehicles.

Analysis of passenger travel time results

This paper takes into account two travel modes, namely the dynamic detour ride-sharing mode and the single-ride mode, and conducts experiments. The travel times of passengers in the two modes are calculated. The distribution of each passenger's travel time is shown in *Figure 8*.

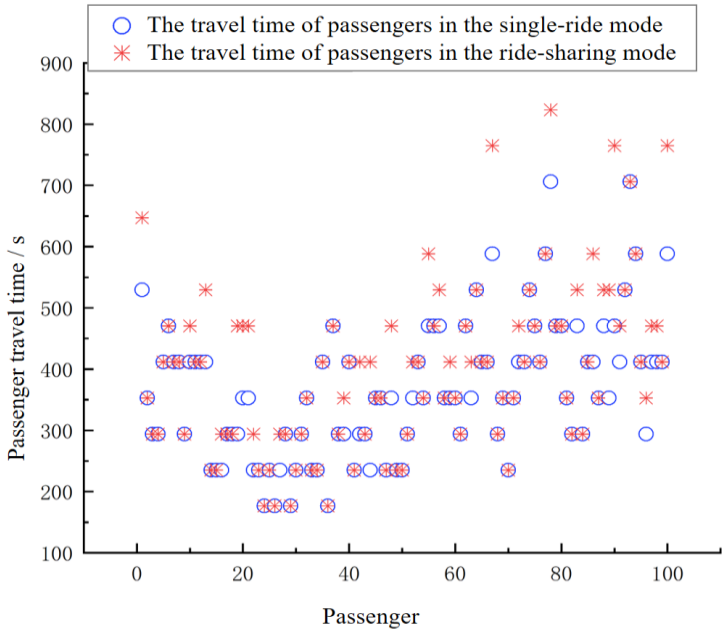

Figure 8 – Passenger travel time distribution

In *Figure 8*, the red symbols represent the travel times of passengers in the ride-sharing mode, while the blue symbols represent those in the single-ride mode. If two symbols overlap, it indicates two situations. Firstly, the ride-sharing routes are highly similar, having no impact on the original travel time. Secondly, the ride-sharing matching fails, and passengers ultimately travel in the single-ride mode. If the travel time in the ride-sharing mode is longer than that in the single-ride mode, it means that this ride-sharing mode is a detour ride-sharing mode. Although passengers' travel times after participating in ride-sharing are greater than or equal to those in the single-ride mode, they are all within a reasonable range. If the detour time is within the acceptable range of passengers and does not harm the interests of the operator, it shows that the dynamic detour ride-sharing mode can serve more passengers with fewer vehicles. This can not only reduce the costs for both passengers and the operator but also effectively relieve traffic congestion.

Total vehicle mileage under dynamic detour ride-sharing mode and single-ride mode

Based on the ride-sharing mode and the single-ride mode, the total mileage L_1 and total mileage L_2 of SAVs are analysed respectively, and the results are shown in *Figure 9*.

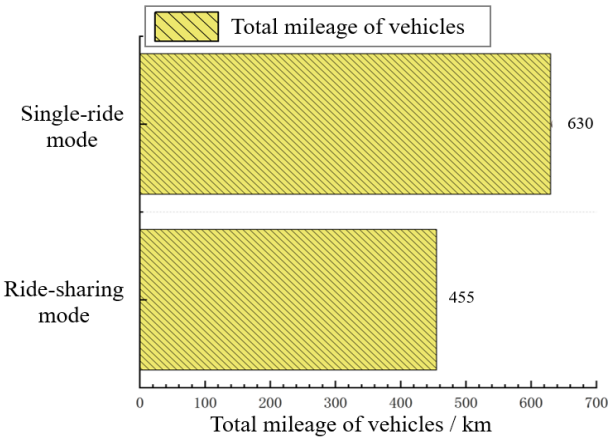

Figure 9 – Number of vehicles and total mileage in ride-sharing and single-ride modes

As can be seen from *Figure 9*, the total mileage of vehicles in the ride-sharing mode is 455 km, while that in the single-ride mode is 630 km. The total mileage of vehicles in the ride-sharing mode is significantly lower than that in the single-ride mode. Using the $\phi = 1 - L_1 / L_2$ formula, it is found that the profit margin of the operator in the ride-sharing mode is 27.8% higher than that in the single-ride mode, indicating that the benefits of the ride-sharing mode are notably improved. By considering the real-time scheduling of SAVs for dynamic ride-sharing, SAVs can receive passengers' ride-sharing requests in real-time and provide ride-sharing services for multiple passengers in one vehicle. This avoids the increase in the driving mileage of SAVs caused by separately dispatching empty vehicles, thus preventing resource waste.

3.3 Discussion on experimental simulation results

On the ride-sharing rate and the number of vehicles in different ride-sharing modes

The combination rate and the number of vehicles required by the dynamic detour combination and overlapping combination modes are quite different. This is because the dynamic detour combination mode is not limited to the same destination and provides a more flexible combination route on the premise of meeting the detour combination mileage, taking passengers from different travel routes into account, and providing more opportunities for passengers to travel together. With the same number of trips, the number of vehicles required will decrease due to the increase in the number of people participating in ride-sharing. Therefore, dynamic detour ride-sharing can serve more passengers with fewer vehicles.

On the travel time under the dynamic detour ride-sharing mode and single ride mode

Under the dynamic detour ride-sharing mode, the travel time of passengers is greater than or equal to the travel time of the single ride mode. Dynamic detour ride-sharing may generate detour mileage and increase travel time. If the passengers' ride-sharing mode belongs to the overlap ride-sharing mode, that is, the similarity of travel routes between passengers participating in ride-sharing is high, their travel time will not be affected. Although the roundabout ride will increase the travel time of passengers, it is within the acceptable range for passengers. The results show that the dynamic ride around mode can use fewer vehicles to serve more passengers, which can not only reduce the cost of passengers and operators but also alleviate traffic congestion.

On the total mileage of vehicles in the dynamic detour combined mode and single mode

The total mileage in the dynamic detour ride-sharing mode is much lower than that in the single ride mode. Considering the real-time scheduling of SAVs with dynamic ride-sharing, SAVs can receive passengers' ride-sharing requests in real time, provide ride-sharing travel services for multiple people in one vehicle, and avoid increasing the mileage of SAVs due to separate scheduling of empty vehicles, resulting in a waste of resources.

4. PARAMETER SENSITIVITY ANALYSIS

4.1 Trend analysis of the variation of uncertainties with cost deviation factors

Set the value range of the cost deviation factor β as 0.01~0.1, calculate the expected target values $(1 + \beta^{RM})T_0$ and $(1 - \beta^{OM})T_0$ of the RM and the OM, and calculate the uncertainty α^{RM} and α^{OM} and the travel time cost of passengers, as shown in *Table 5*. The variation trend of uncertainty α^{RM} and α^{OM} and passenger travel time cost with β^{RM} and β^{OM} is shown in *Figure 10*. According to the calculation of the real-time scheduling model, the base value T_0 of the total travel time cost of passengers is 665 min.

Table 5 – α^{RM} and α^{OM} and the travel time cost of passengers

β^{OM}、β^{RM}	RM		OM	
	α^{RM}	**Travel time cost of passengers**	α^{OM}	**Travel time cost of passengers**
0.01	0.01	671.65	0.01	658.35
0.02	0.02	678.30	0.02	651.70
0.03	0.03	684.95	0.03	645.50
0.04	0.04	691.60	0.04	638.40
0.05	0.05	698.25	0.05	631.75
0.06	0.06	704.90	0.06	625.10
0.07	0.07	711.55	0.07	618.45
0.08	0.08	718.20	0.08	611.80
0.09	0.09	724.85	0.09	605.15
0.1	0.1	731.5	0.1	598.50
0.01	0.01	671.65	0.01	658.35

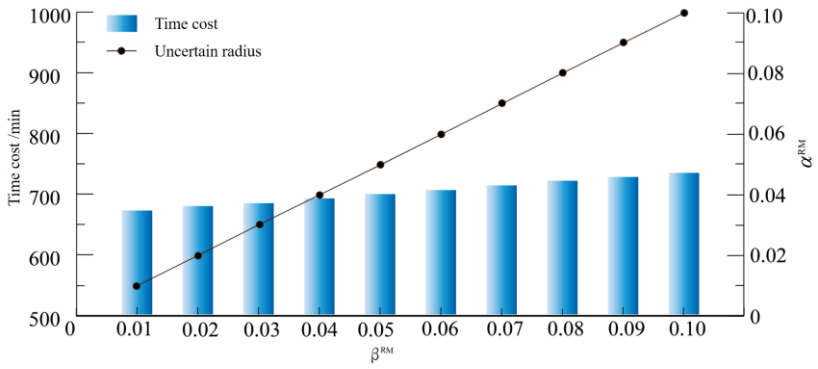

(a)

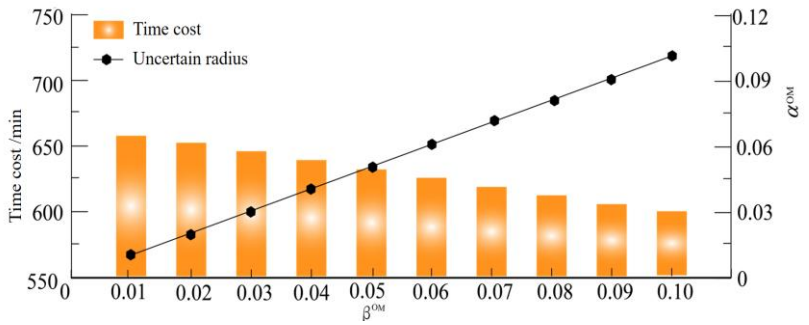

(b)

Figure 10 – Variation trend of travel time cost of uncertain radius α^{RM} and α^{OM} and passengers: a) RM; b) OM

It can be seen from *Figure 10* that in the RM model, the uncertainty α^{RM} increases with the increase of the deviation factor, and the travel time cost of passengers increases. This is because in RM, decision makers believe that the uncertainty of passenger travel time plays a negative role in reducing the travel time cost of passengers. The greater the α^{RM}, the smaller the impact of uncertainty on the travel time cost of passengers, that is, the better the robustness. No matter how the travel time of passengers changes within the $\left[(1-\alpha^{RM})\ t_{ij}^{*},(1+\alpha^{RM})\ t_{ij}^{*}\right]$ range, the travel time cost of passengers can be lower than the expected value

$(1+\beta^{RM})T_0$. In the OM model, the uncertainty radius α^{OM} increases with the increase of the deviation factor, and the travel time cost of passengers decreases. This is because decision makers believe that the uncertainty of passenger travel time plays a positive role in reducing the travel time cost of passengers. The greater the α^{OM}, the more obvious the reduction of travel time cost caused by travel time uncertainty. No matter how the travel time of passengers changes within the scope of $\left[(1-\alpha^{OM})\, t_{ij}^{*}, (1+\alpha^{OM})\, t_{ij}^{*}\right]$, the travel time cost of passengers can be lower than the expected value $(1-\beta^{OM})T_0$.

4.2 Sensitivity analysis of cycle duration to ride-sharing rate

To analyse the impact of cycle duration on the ride-sharing rate, we assume that the cycle duration t_0 is 90 s and 120 s, respectively, and keep other parameters unchanged. Then we solve the real-time dispatching model of shared autonomous vehicles in the ride-sharing mode. The results related to the ride-sharing rate are shown in *Figure 11*.

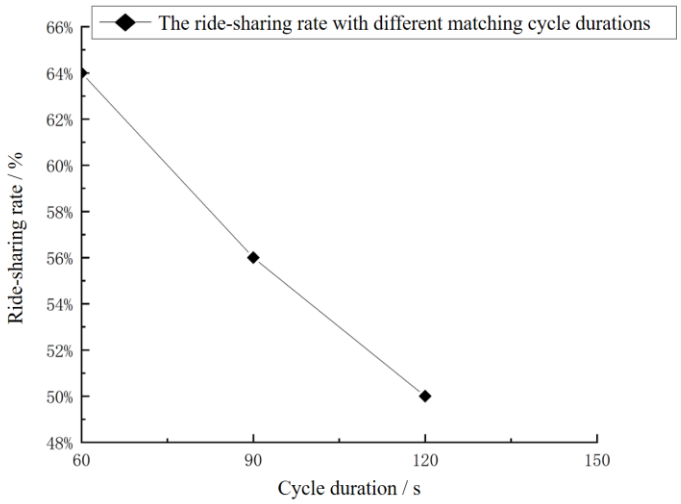

Figure 11 – The ride-sharing rate with different matching cycle durations

It can be seen from *Figure 11* that the shorter the cycle time, the higher the ride-sharing rate. This is because the shorter the cycle time, the faster the system refreshes the passenger request information. The more times the passenger requests for information are refreshed, the greater the chance of securing a ride in a match. The longer the cycle length, the more passengers' requests occur within the same cycle, and passengers in that cycle cannot carry out internal ride-sharing, resulting in a decrease in the ride-sharing rate.

5. CONCLUSION

This paper addresses the ride-sharing scheduling issue for shared autonomous vehicles (SAVs) and introduces a dynamic detour ride-sharing mode. The goal is to minimise total travel time costs for passengers while maximising the ride-sharing distance ratio. We construct a real-time scheduling model for SAVs in ride-sharing mode and propose a solution for this model. Utilising information gap decision theory, we analyse the robustness and opportunism of the real-time scheduling model. Based on the findings of this study, we draw the following conclusions:

— This paper proposes a real-time scheduling model and its solution for SAVs in ride-sharing mode. Through experimental simulations, it is found that the passenger ride-sharing rate in the dynamic detour ride-sharing mode is higher than in the overlapping ride-sharing mode, and the ride-sharing benefits are significantly improved, indicating that the model and its solution are effective.

— Compared to the SAV scheduling model that solely considers overlapping ride-sharing, the dynamic detour ride-sharing scheduling model, which takes into account passengers' ride-sharing preferences, offers greater flexibility. It does not constrain passengers' starting and ending points, nor is it limited to specific routes, making it more adaptable to the diverse travel needs of travellers. To minimise total travel time costs (minimising passengers' total travel time) and maximising the ride-sharing distance ratio, it can meet the interests of both operators and passengers.

— The simulation experiment of the model shows that under the detour ride-sharing mode, the ride-sharing rate of the dispatched SAVs is 64%, with 68 vehicles required. This ride-sharing rate is 22% higher than that under the overlapping ride-sharing mode, and the number of vehicles is reduced by 11. It can be inferred that if the detour time is within passengers' acceptable range and does not harm the interests of the operator, then the dynamic detour ride-sharing mode is conducive to promoting passenger ride-sharing, reducing travel energy consumption, and alleviating traffic congestion.
— Through the analysis of the variation trend of the uncertainty of travel time with the cost deviation factors, the robustness of the model increases as total travel time costs rise. That is, the robustness of the model is enhanced by increasing costs. Meanwhile, the opportunity degree increases as total travel time costs decrease. The operator can conduct a risk assessment and determine their risk preference regarding interests, then decide on the real-time scheduling plan based on the robustness and opportunity degree of the model.

REFERENCES

[1] Santhanakrishnan N, Emmanouil C, Constantinos A. Shared autonomous vehicle services: A comprehensive review. *Transportation Research Part C: Emerging Technologies*. 2020;111:255-293. DOI: 10.1016/j.trc.2019.12.008.

[2] Rongjie Y, Ye T, Jian S. Highly automated vehicle virtual testing: A review of recent developments and research frontiers. *China Journal of Highway and Transport*. 2020;33(11):125-138. DOI: 10.19721/j.cnki.1001-7372.2020.11.011.

[3] Zhuoping Y, Xingyu X, Junyi C. Review on automated vehicle testing technology and its application. *Journal of Tongji University (Natural Science)*. 2019;47(4):540-547. DOI: 10.11908/j.issn.0253-374x.2019.04.013.

[4] Karolemeas C, et al. Shared autonomous vehicles and agent-based models: A review of methods and impacts. *Eur. Transp. Res. Rev*. 2024;25:16. DOI: 10.1186/s12544-024-00644-2.

[5] Prashanth V, Michael WL. A congestion-aware Tabu search heuristic to solve the shared autonomous vehicle routing problem. *Journal of Intelligent Transportation Systems*. 2021;25(4):343-355. DOI: 10.1080/15472450.2019.1665521.

[6] Becker F, Axhausen KW. Literature review on surveys investigating the acceptance of automated vehicles. *Transportation*. 2017;44(6):1293-1306. DOI: 10.1007/s11116-017-9808-9.

[7] Doina O, et al. Peer-to-Peer (P2P) carsharing and driverless vehicles: Attitudes and values of vehicle owners. *Transportation Research Part A: Policy and Practice*. 2021;151:180-194. DOI: 10.1016/j.tra.2021.07.008.

[8] Paddeu D, et al. A study of users' preferences after a brief exposure in a Shared Autonomous Vehicle (SAV). *Transportation Research Procedia*. 2021;52(6):533-540. DOI: 10.1016/j.trpro.2021.01.063.

[9] Krueger R, Rashidi TH, Rose JM. Preferences for shared autonomous vehicles. *Transportation Research Part C: Emerging Technologies*. 2019;69:343-355. DOI: 10.1016/j.trc.2016.06.015.

[10] Oama B, et al. Shared autonomous vehicle services and user taste variations: Survey and model applications. *Transportation Research Procedia*. 2020;47:3-10. DOI: 10.1016/j.trpro.2020.03.066.

[11] Alexandra K, Jan G. Travellers' willingness to share rides in autonomous mobility on demand systems depending on travel distance and detour. *Travel Behaviour and Society*. 2020;21:188-202. DOI: 10.1016/j.tbs.2020.06.010.

[12] Pourgholamali M, et al. Sustainable deployment of autonomous vehicles dedicated lanes in urban traffic networks. *Sustainable Cities and Society*. 2023;99:104969. DOI: 10.1016/j.scs.2023.104969.

[13] Panick K, et al. Autonomous taxis and ride-sharing vehicles: A social construct perspective for future mobility and infrastructure readiness. *Sustainable Cities and Society*. 2025;118:106060. DOI: 10.1016/j.scs.2024.106060.

[14] Gkartzonikas C, Ke Y, Gkritza K. A tale of two modes: Who will use single user and shared autonomous vehicles. *Case Studies on Transport Policy*. 2022;10(3):1566-1580. DOI: 10.1016/j.cstp.2022.05.015.

[15] Ronghan Y, et al. Empirical analysis of choice behavior for shared autonomous vehicles with concern of ride-sharing. *Journal of Transportation Systems Engineering and Information Technology*. 2020;20(1):228-233. DOI: 10.16097/j.cnki.1009-6744.2020.01.033.

[16] Mohammadhossein A, et al. Unravelling interrelationships and moderators influencing the acceptance of shared autonomous vehicles: An end users' perspective. *Transportation Research Part F: Traffic Psychology and Behaviour*. 2025;113:158-173. DOI: 10.1016/j.trf.2025.04.002.

[17] Ouaïl AM, et al. Shared autonomous vehicle services and user taste variations: survey and model applications. *Transportation Research Procedia*. 2020;47:3-10. DOI: 10.1016/j.trpro.2020.03.066.

[18] Zihe Z, et al. Charging infrastructure assessment for shared autonomous electric vehicles in 374 small and medium-sized urban areas: An agent-based simulation approach. *Transport Policy*. 2024;155:58-78. DOI: 10.1016/j.tranpol.2024.06.017.

[19] Zihe Z, et al. Shared low-speed autonomous vehicles for short-distance trips: agent-based modeling with mode choice analysis. *Transportation Planning and Technology*. 2024;48(2):313-341. DOI: 10.1080/03081060.2024.2373322.

[20] Mehdi N, Matthew JR. Agent based model for dynamic ridesharing. *Transportation Research Part C: Emerging Technologies*. 2016;64:117-132. DOI: 10.1016/j.trc.2015.07.016.

[21] Mohamadhossein N, Bo Z. One-to-many matching and section-based formulation of autonomous ridesharing equilibrium. *Transportation Research Part B: Methodological*. 2022;155:72-100. DOI: 10.1016/j.trb.2021.11.002.

[22] Chengqi L, et al. Multi-Agent reinforcement learning framework for addressing Demand-Supply imbalance of Shared Autonomous Electric Vehicle. *Transportation Research Part E: Logistics and Transportation Review*. 2025;197:104062. DOI: 10.1016/j.tre.2025.104062.

[23] Hyland M, Mahmassani HS. Dynamic autonomous vehicle fleet operations: Optimization-based strategies to assign AVs to immediate traveller demand requests. *Transportation Research Part C: Emerging Technologies*. 2018;92:278-297. DOI: 10.1016/j.trc.2018.05.003.

[24] Qian G, Ke H, Xiaobo L. Matching and routing for shared autonomous vehicles in congestible network. *Transportation Research Part E: Logistics and Transportation Review*. 2021;156:102513. DOI: 10.1016/j.tre.2021.102513.

[25] Masoud N, Jayakrishnan R. A real-time algorithm to solve the peer-to-peer ride-matching problem in a flexible ridesharing system. *Transportation Research Part B: Methodological*. 2017;106:218-236. DOI: 10.1016/j.trb.2017.10.006.

[26] Yantao H, Kara MK, Venu G. Shared automated vehicle fleet operations for first-mile last-mile transit connections with dynamic pooling. *Computers, Environment and Urban Systems*. 2022;92:101730. DOI: 10.1016/j.compenvurbsys.2021.101730.

[27] Zhimian W, Kun A, Gonçalo C, et al. Real-time scheduling and routing of shared autonomous vehicles considering platooning in intermittent segregated lanes and priority at intersections in urban corridors. *Transportation Research Part E: Logistics and Transportation Review*. 2024;186:103546. DOI: 10.1016/j.tre.2024.103546.

[28] Ben HY. Information gap decision theory. *Decision Making under Deep Uncertainty*. 2019:93-115. DOI: 10.1007/978-3-030-05252-2_5.

[29] Kuhn HW. The Hungarian method for the assignment problem. *Naval Research Logistics Quarterly*. 1955;2(1):83-97. DOI: 10.1002/nav.3800020109.

[30] Chopra S, et al. A distributed version of the hungarian method for multirobot assignment. *IEEE Transactions on Robotics*. 2017;1-16. DOI: 10.1109/TRO.2017.2693377.